GeoConvention 2015
GEOSCIENCE
new horizons
Telus Convention Centre • 4-8 May 2015 • Calgary, AB Canada

Vector imaging of converted wave seismic data

Aaron Stanton and Mauricio D. Sacchi

Department of Physics, University of Alberta

Summary

One way wave equation migration of elastic data generally consists of wavefield separation, extrapolation, and an imaging condition. In isotropic media wavefield separation is achieved via Helmholtz decomposition. Implementing Helmholtz decomposition at the receiver datum (typically at a boundary) is problematic. We propose an alternative approach where all components of the data are extrapolated using both P and S-wave velocities thereby creating vector PP and PS images. Poynting vectors computed from the source and receiver side wavefields are used to bin migrated shot gathers into angle bins as well as to perform a polarization correction prior to summing the vector images. Cross talk artifacts persist in the PP and PS images but are somewhat mitigated by the polarization correction and can be further removed by Radon or FK filtering of angle gathers. The method could be used to avoid wavefield separation in the complicated near surface or in cases where initial estimates of P and S-wave velocities are not accurate enough to properly separate wavefields for converted wave velocity analysis.

Introduction

Migration of converted wave data is hampered by the wavefield separation step where P and S wave potentials must be extracted from data components prior to imaging. An alternative formulation was first proposed by Hou and Marfurt in 2002 in which data components are migrated and the separation is dealt with after the imaging condition by calculating polarization angles at each point in the models from the components of the migrated shot gathers. We propose an alternative formulation in which polarization angles are calculated directly from the source and receiver side wavefields using Poynting vectors.

Theory

Migration of two component elastic data by one way wave equation migration can be written

$$\begin{bmatrix} \tilde{\mathbf{m}}_{pp} \\ \tilde{\mathbf{m}}_{ps} \end{bmatrix} = \begin{bmatrix} \mathbf{L}_{pp}^{T} & \mathbf{0} \\ \mathbf{0} & \mathbf{L}_{ps}^{T} \end{bmatrix} \mathbf{H} \begin{bmatrix} \mathbf{d}_x \\ \mathbf{d}_z \end{bmatrix} \tag{1}$$

where $\mathbf{H}$ denotes Helmholtz decomposition of vector displacements into P and S scalar potentials. Here $\mathbf{L}_{\mathbf{pp}}^{\mathbf{T}}$ is a shot profile split step forward migration operator (Stoffa et al., 1990) that uses the P-wave velocity for both the source and receiver side wavefields (conversely the operator $\mathbf{L}_{\mathbf{ps}}^{\mathbf{T}}$ uses the P-wave velocity for the source side wavefield and the S-wave velocity for the receiver side wavefield). Alternatively, to avoid the need for Helmholtz decomposition the migration can be formulated as

$$\begin{bmatrix} \tilde{\mathbf{m}}_{pp} \\ \tilde{\mathbf{m}}_{ps} \end{bmatrix} = \begin{bmatrix} sgn(\theta) \cdot cos|\theta| & sin|\theta| & \mathbf{0} & \mathbf{0} \\ \mathbf{0} & \mathbf{0} & sgn(\theta) \cdot sin|\theta| & cos|\theta| \end{bmatrix} \begin{bmatrix} \mathbf{L}_{pp}^{T} & \mathbf{0} \\ \mathbf{0} & \mathbf{L}_{pp}^{T} \\ \mathbf{L}_{ps}^{T} & \mathbf{0} \\ \mathbf{0} & \mathbf{L}_{ps}^{T} \end{bmatrix} \begin{bmatrix} \mathbf{d}_x \\ \mathbf{d}_z \end{bmatrix} \tag{2}$$

where the angle θ denotes the polarization of the vector components of the image. The polarization matrix in equation 2 adds contributions of the 4 vector images to the final images $\tilde{\mathbf{m}}_{pp}$ and $\tilde{\mathbf{m}}_{ps}$ and

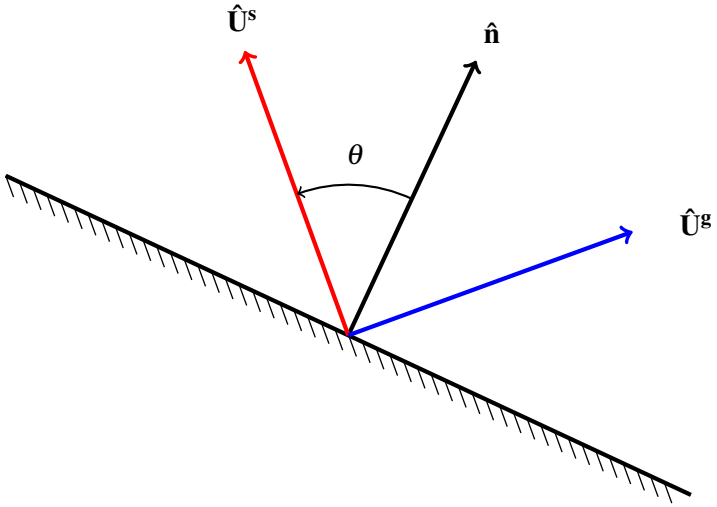

Figure 1 *Schematic displaying source ($\hat{\mathbf{U}}^{\mathbf{s}}$) and receiver side ($\hat{\mathbf{U}}^{\mathbf{g}}$) Poynting vectors relative to the reflector normal ($\hat{\mathbf{n}}$).*

corrects for converted wave polarity reversal that occurs at normal incidence to a reflector. To find the polarization angles for every point in an image for a given shot gather, Hou and Marfurt (2002) solved for the angles directly from vector images (for example $\theta = tan^{-1}(\frac{\mathbf{m}^x_{pp}}{\mathbf{m}^z_{pp}})$). In our formulation we obtain polarization angles directly from Poynting vectors calculated during the PP extrapolation of the data.

Poynting vectors are calculated via $S_i = -\tau_{ij}\dot{u}_j$ where $\mathbf{u}$ is the particle displacement and τ_{ij} is the stress tensor (Dickens and Winbow, 2011). This can be approximated by $\mathbf{S} \approx \bigtriangledown P \frac{\partial P}{\partial t} P$ where P is the pressure (Yoon and Marfurt, 2006). Higginbotham et al. (2010) outline a strategy to compute angle gathers in wave equation migration. First the gradient components for the source side wavefield are computed as $U^s_x(w,k_x,k_z) = k_x U^s(w,k_x,k_z)$. Next obtain $U^s_x(x,z)$ that corresponds to the time of reflection by calculating the zero-lag cross correlation with the receiver wavefield: $U^s_x(x,z) = \int U^s_x(w,x,z)U^{g^*}(w,x,z)d\omega$. Lastly normalize the elements of $U^s(x,z) = U^s_x(x,z)\hat{\mathbf{x}} + U^s_z(x,z)\hat{\mathbf{z}}$ and repeat the process for the z-component of the source side wavefield to obtain $U^s_z(x,z)$.

These steps are repeated for the x and z components of the receiver side wavefield to obtain the unit vectors: $\hat{\mathbf{U}}^s(x,z)$, and $\hat{\mathbf{U}}^g(x,z)$. In practice we find that we must multiply $U^s_x(x,z)$ by -1 to obtain unit vectors following the convention shown in figure 1. Using these vectors we may calculate the angle of incidence with respect to the reflector normal as $\theta(x,z) = \frac{1}{2}cos^{-1}\left(\hat{\mathbf{U}}^s(x,z)\cdot\hat{\mathbf{U}}^g(x,z)\right)$. For 2D imaging the signed incidence angle can be found by multiplying by the sign of the cross product: $\theta(x,z) = sgn\left(\hat{\mathbf{U}}^s(x,z)\times\hat{\mathbf{U}}^g(x,z)\right)\frac{1}{2}cos^{-1}\left(\hat{\mathbf{U}}^s(x,z)\cdot\hat{\mathbf{U}}^g(x,z)\right)$ while for 3D imaging we can compute the reflection azimuth (Dickens and Winbow, 2011).

The incidence angles with reference to the reflector normal for each migrated shot $\tilde{\mathbf{m}}^x_{pp}$, $\tilde{\mathbf{m}}^z_{pp}$,$\tilde{\mathbf{m}}^x_{ps}$, $\tilde{\mathbf{m}}^z_{ps}$ are used to interpolate the data into angle bins and correct for the polarization to create the final images $\tilde{\mathbf{m}}_{pp}$ and $\tilde{\mathbf{m}}_{ps}$ according to equation 2.

Example

To demonstrate the method we generated 50 synthetic two component shot gathers via elastic finite difference modelling over a 3-layer model. X and Z-components for a single shot located at X=3500m are shown in figure 2. The shot gathers were migrated using the proposed method into 37 angle bins ranging from -90 to 90° with an increment of 5°.

Stacked PP and PS images (windowed from -45 to 45° prior to stacking) are shown in figure 3.

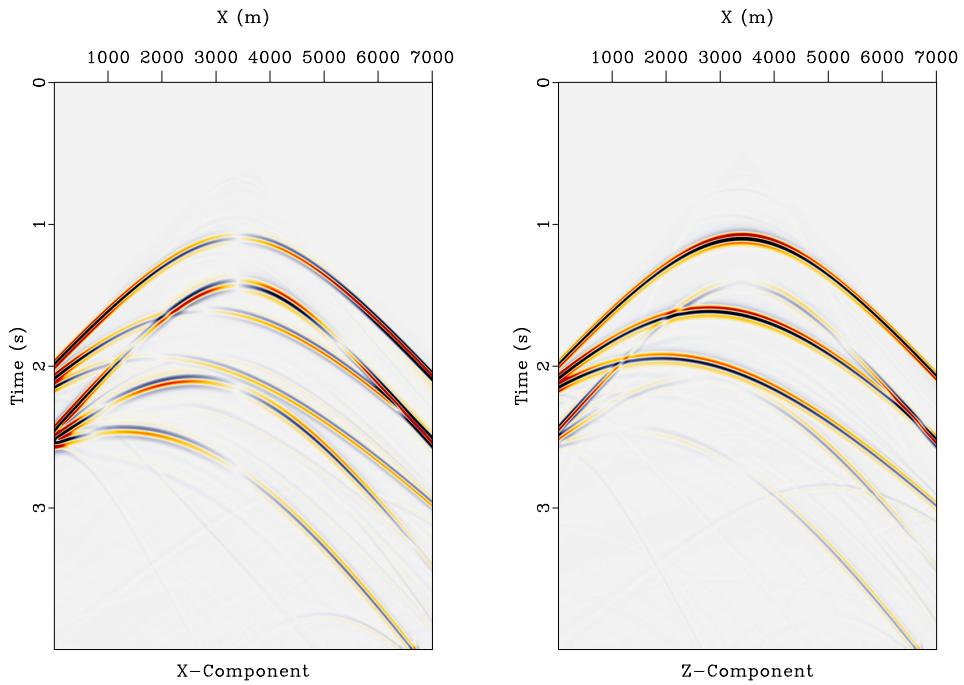

Figure 2 *Elastic finite difference synthetic shot gather generated over a 3-layer model the shot is located at X=3500m. 50 shot gathers were generated over the model to test the migration.*

Note that there is minimal cross-talk energy in the PP section (top of figure 3) despite the fact that the algorithm does not incorporate a wavefield separation step. The weak PS cross-talk energy (migrated with too high a velocity) is positioned lower than the true reflector position. The polarization correction applied to the vector images prior to summing them (equation 2) has also minimized much of the PS crosstalk energy. In the PS section (bottom of figure 3) the PP crosstalk energy is slightly stronger in amplitude but still much weaker than the PS energy. In this case the PP energy has been migrated with too low a velocity placing the energy above the true reflector position. Looking at the angle gathers (figure 4), we see that the PP crosstalk energy in the PS gather has hyperbolic moveout and could be further attenuated by Radon or FK filtering of the angle gathers.

Conclusion

We introduced a method to migrate elastic data that avoids the wavefield separation step. Data components are migrated using P and S-wave velocity fields and a polarization correction is applied to the vector images prior to summing them. The polarization angles are computed directly from the source and receiver side wavefields using Poynting vectors. We find that the approach leads to minimal PS cross talk in the PP image, while the PS image displays slightly more PP crosstalk energy that could be further attenuated by Radon or FK filtering of angle gathers.

Acknowledgements

The authors are grateful to the sponsors of Signal Analysis and Imaging Group (SAIG) at the University of Alberta.

References

Dickens, T. and G. Winbow, 2011, Rtm angle gathers using poynting vectors: Presented at the 2011 SEG Annual Meeting.
Higginbotham, J., M. Brown, and C. Macesanu, 2010, Depth migration velocity model building with wave equation imaging: First Break, **28**, 27–33.
Hou, A. and K. J. Marfurt, 2002, Multicomponent prestack depth migration by scalar wavefield extrapolation: Geophysics, **67**, 1886–1894.
Stoffa, P. L., J. T. Fokkema, R. M. de Luna Freire, and W. P. Kessinger, 1990, Split-step fourier migration: Geophysics, **55**, 410–421.
Yoon, K. and K. J. Marfurt, 2006, Reverse-time migration using the poynting vector: Exploration Geophysics, **37**, 102–107.

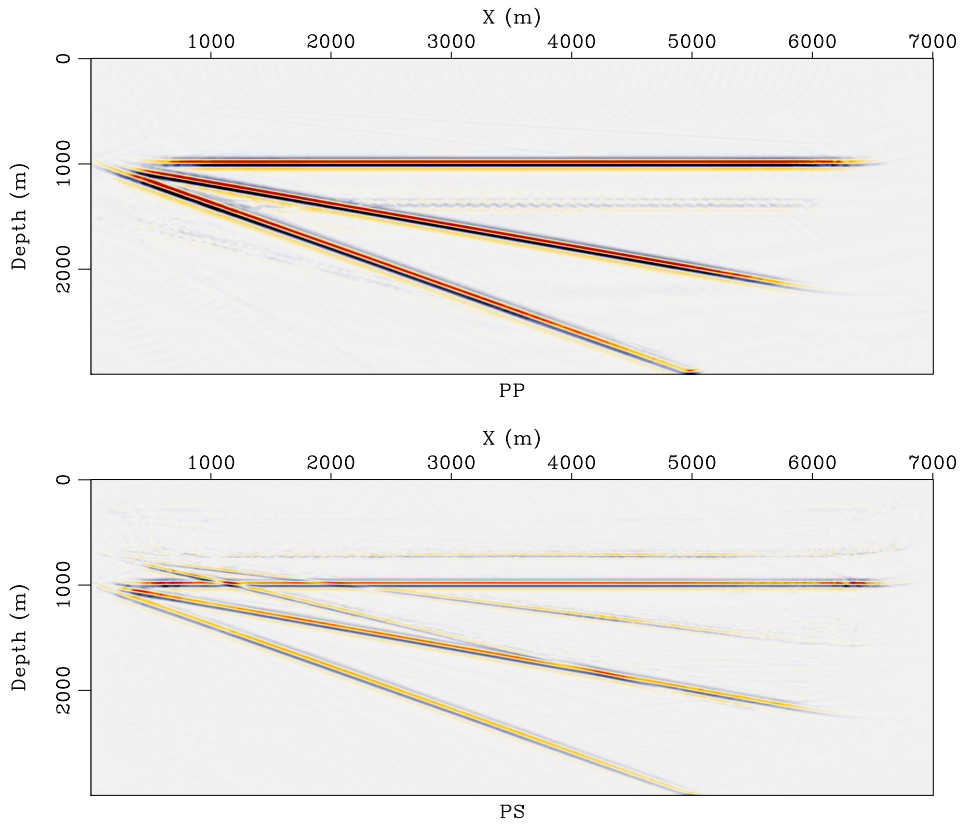

Figure 3 *PP and PS stacked images generated using the proposed method. Incidence angles from -45 to 45° (relative to reflector normal) were stacked.*

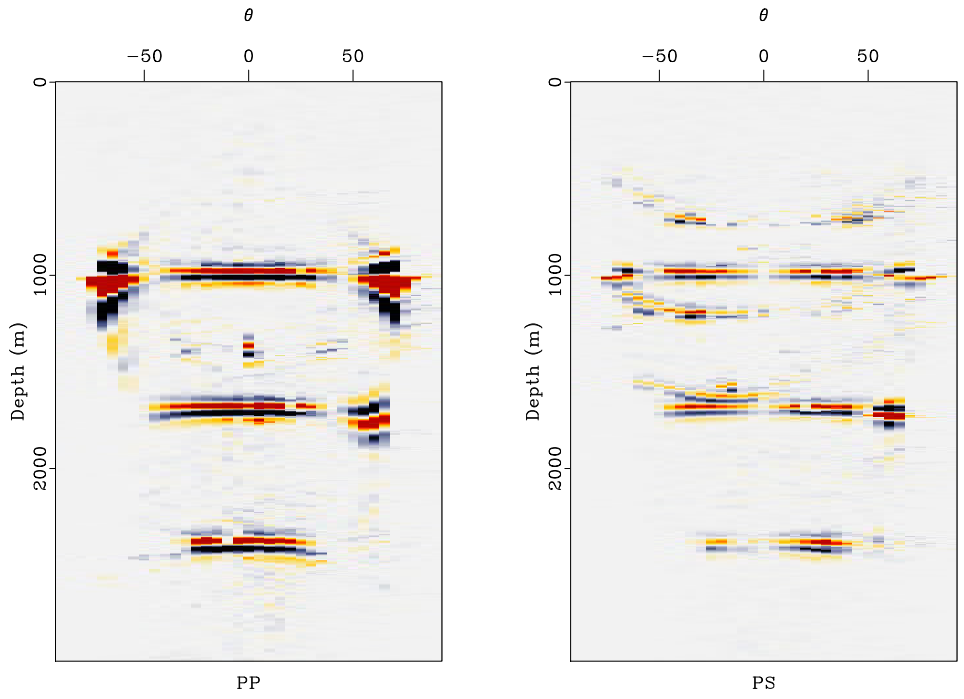

Figure 4 *PP and PS angle gathers for X=3500m generated using the proposed method.*